

Gripe water-mediated green synthesis of silver nanoparticles and their applications in nonlinear optics and surface-enhanced Raman spectroscopy

E. Kirubha · K. Vishista · P. K. Palanisamy

Received: 18 July 2014 / Accepted: 25 October 2014 / Published online: 8 November 2014
© The Author(s) 2014. This article is published with open access at Springerlink.com

Abstract In the present study, silver nanoparticles were synthesized from aqueous silver nitrate through a simple, eco-friendly and ‘green’ method using gripe water as reducing as well as stabilizing agent. Control over the dispersity of silver (Ag) nanoparticles was attained by altering the synthesis process. The size and morphology of the particles were perceived using high-resolution transmission electron microscope and the surface plasmon resonance of the prepared nanoparticles was observed by UV–VIS spectrum. Herein, we report the nonlinear optical behavior and surface-enhanced Raman spectroscopy of silver nanoparticles with different particle size and dispersity. The nonlinear optical behavior was studied by single beam Z-scan technique using tunable Ti: Sapphire mode-locked femtosecond laser as source. The nonlinear optical parameters such as the nonlinear refractive index, nonlinear absorption coefficient β and the third-order nonlinear susceptibility χ^3 of the prepared Ag nanoparticles were obtained for various wavelengths by tuning the wavelength of the laser from 700 to 950 nm. Surface-enhanced Raman spectroscopy (SERS) is an inspiring phenomenon especially in the case of silver nanoparticles. The as-synthesized silver nanoparticles show huge enhancements in the order of 10^9 in the Raman spectrum of rhodamine 6G dye.

Keywords Silver nanoparticles · Nonlinear optics · Z-scan · SERS · Gripe water

E. Kirubha · K. Vishista
Department of Physics, Anna University, Chennai, India

P. K. Palanisamy (✉)
Department of Medical Physics, Anna University, Chennai, India
e-mail: profpkp@yahoo.com

Introduction

Metal nanoparticles have gained interest mainly because of their size- and shape-dependent electronic and optical properties (Kelly et al. 2003). Although tailoring the size and shape of the nanoparticles for a required application is always challenging, metal nanoparticles have found a wide range of applications in catalysis (Lakshmi pathy et al. 2014; Venkatesham et al. 2014), photonics and optoelectronics (Maier et al. 2003; Sun and Xia 2002). In medical field they are also used in biosensing (Anker et al. 2008), biolabeling (Junhua et al. 2009), drug delivery (Liong et al. 2008) and cancer diagnosis and treatment (Sayed et al. 2005; Jeyaraj et al. 2013). Owing to the anti-bacterial activity of Ag nanoparticles, they are used as coating in medical devices and also in burn ointments (Atiyeh et al. 2007). A number of methods have come up for the preparation of gold and silver nanoparticles including electrochemical reduction, photochemical reduction (Pourjavadi and Soleyman 2011) and laser irradiation (Mafuné et al. 2000). Silver nanoparticles with uniform size are usually synthesized using the conventional chemical reduction methods using reducing agents such as sodium borohydride and sodium citrate (Dong et al. 2010). However, there is a growing need of the green synthesis techniques for the preparation of nanoparticles. The ‘green’ synthesis protocols are advantageous over the chemical reduction techniques as they are less toxic, eco-friendly and economical. Ag nanoparticles have been synthesized using microorganisms such as algae (Singh et al. 2013), bacteria (Mohanpuria et al. 2008), and fungi (Honary et al. 2013). Various green synthesis procedures for the synthesis of gold and silver nanoparticles have evolved using plant extracts (Vankar and Shukla 2012; Augustine et al. 2013; Swamy et al.

2014; Majumdar and Bag 2013), fruit (Dauthal and Mukhopadhyay 2013) and flower extracts (Philip 2010). The three main factors of complete green synthesis of Ag nanoparticles on green chemistry perspectives include the selection of solvent, environmentally benign reducing agent and the selection of nontoxic stabilizing agents (Raveendran et al. 2003).

In this study, we report a complete green synthesis of Ag nanoparticles using gripe water as environmentally benign reducing as well as nontoxic stabilizing agent adopting the procedure followed for the synthesis of Au nanoparticles (Kirubha and Palanisamy 2013). The dispersity of nanoparticles was controlled by this technique as both monodispersed and polydispersed Ag nanoparticles were produced using gripe water at room temperature (25 °C). Gripe water is a well-known, antacid generally prescribed for children to treat indigestion, gripe and acidity (Blumenthal 2000). In this reported work, we have used Woodward's gripe water. It is easily available in medical stores all over the world. We also report the nonlinear optical behavior and the SERS performance of the prepared silver nanoparticles. Using single beam Z-scan technique, the nonlinear refractive index n_2 , nonlinear absorption coefficient β and the third-order nonlinear susceptibility of the χ^3 were studied and measured for different wavelengths varying from 700 to 900 nm using Ti:Sapphire mode-locked femtosecond laser.

Surface-enhanced Raman spectroscopy discovered in the early 1970s (Fleishman et al. 1974; Janmaire and Duynes 1977) is a valuable tool for chemical and biological sensing due to its high sensitivity and precision. The molecules in close contact with metallic nanoparticles enhance the Raman signal to several orders of magnitude. SERS occurs due to two main mechanisms: (1) electromagnetic and (2) chemical of which the main contribution is due to the electromagnetic mechanism (Moskovits 2005). Silver nanoparticles are extensively used in SERS studies as they serve as good substrate to enhance the Raman signals. In this study, we also report the surface-enhanced Raman scattering of the rhodamine 6G by varying the dispersity of the as-synthesized Ag nanoparticles.

Experimental

Materials

AgNO₃ was purchased from Sigma-Aldrich and used as such and Woodward's gripe water was purchased from TTK Health Care Ltd., INDIA. For SERS studies, rhodamine 6G was purchased from Sigma-Aldrich.

Synthesis

By adding 5 mL of gripe water to 0.3 mM of AgNO₃, three different samples of Ag nanoparticles were synthesized by varying the stirring time. Sample 1 was prepared by stirring the source solution for the first 1 h, while samples 2 and 3 were prepared by stirring the solution for 6 and 22 h, respectively.

Instrumentation

The surface plasmon bands of the particles were recorded using UV–VIS spectrometer. The absorption spectra for all the particles were recorded using Shimadzu Spectrometer, with a resolution of 0.5 nm taking the nanoparticles in a 10-mm optical length quartz cuvette. The particle size and shape were monitored using high-resolution transmission electron microscope (HR-TEM, JEOL JEM 3010) operated at 200 kV. Samples for TEM images were prepared by placing a drop of colloidal silver on carbon-coated copper grid 300 mesh. The IR spectra were recorded on JASCO FT/IR-4100 Fourier Transform Infrared spectrometer in the range 400–4,000 cm⁻¹ with a resolution of 4 cm⁻¹. The Z-scan studies were performed using a tunable, mode-locked Ti: Sapphire at a repetition rate of 80 MHz with a pulse width of 160 fs laser beam (Mai Tai–Deep SEE) focused by a lens of 32 mm focal length. A photodetector (COHERENT) was connected to the digital power meter Field Master Gs-COHERENT to measure the laser power. The Raman spectra were recorded using LabRAM HR800, Jobin–Yvon, France, with an 80-cm focal length spectrometer and a He–Ne 633 nm with 11 mW power on the sample. The spectra were acquired over a wavenumber region of 1,800–600 cm⁻¹ with an acquisition time of 10 s.

Results and discussion

UV–Visible spectra

The surface plasmon bands (SPR) of the prepared Ag nanoparticles (AgNps) were obtained using the UV–VIS spectra (Fig. 1a). The obtained Ag nanoparticles of samples 1 and 2 (polydispersed as seen from TEM images) exhibit SPR at 413 and 420 nm, respectively, while the nanoparticles of sample 3 (monodispersed as seen from TEM image) exhibit SPR at 405 nm. Broader peaks are observed in the case of polydispersed silver nanoparticles. Figure 1b shows the step by step growth of monodispersed Ag nanoparticles with time. The spectra were recorded for every 15 min and it was observed that up to 45 min there was no formation of nanoparticles as indicated by the flat line, while the spectrum taken after 60 min exhibited SPR

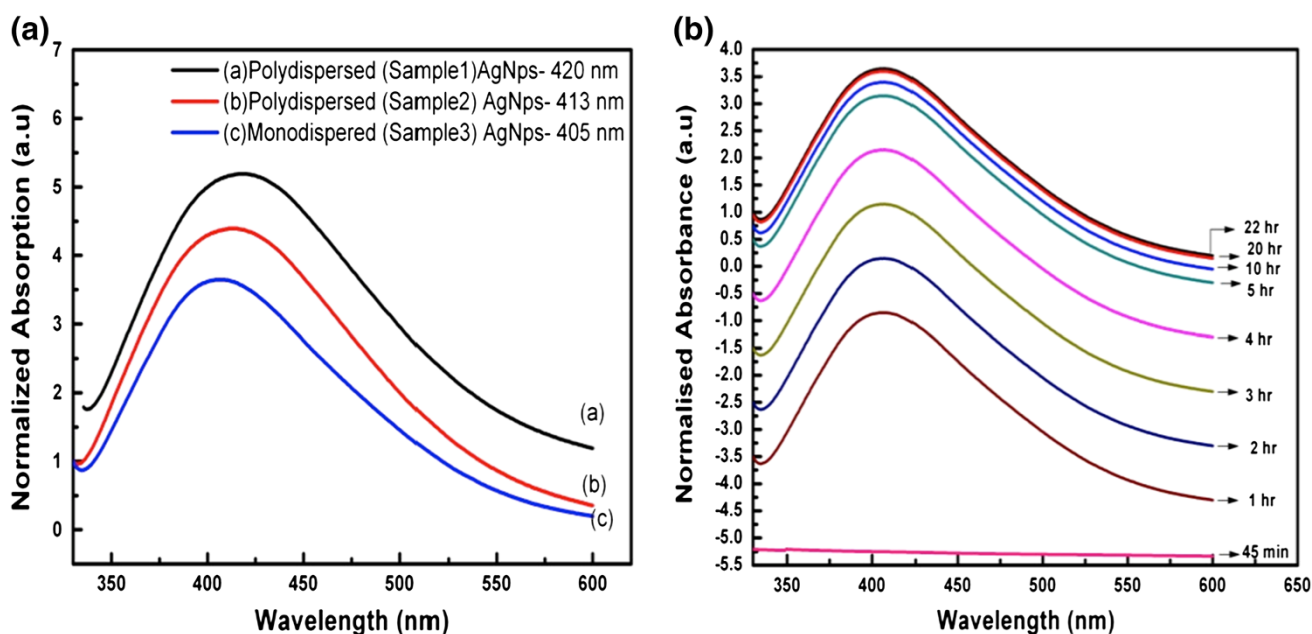


Fig. 1 **a** Surface plasmon band of gripe water reduced polydispersed and monodispersed silver nanoparticles, **b** variation of surface plasmon band of silver nanoparticles with time

band as seen in Fig. 1b. Other spectra taken at 1-h interval exhibited an increase in intensity without any shift in its peak. After 5 h, this increase in intensity also reduced and after 22 h, no change in the intensity was observed indicating that the growth was complete. Observation of no shift in the absorption peak implies that with time the size of the grown nanoparticles did not vary but the number increased.

Transmission electron microscopy

The morphology and the particle size of the nanoparticles thus grown were deduced by high-resolution transmission electron microscope (TEM). The nanoparticles obtained by the stirring the source for the first 1 h (sample 1) resulted with very high polydispersity. The particle size of the Ag nanoparticles of sample 1 varied from 2 to 40 nm as seen in Fig. 2a. The Ag nanoparticles of sample 2 resulted with relatively lesser polydispersity, as the variation in particle size was from 5 to 15 nm. The Ag nanoparticles attained by this process exhibited different shapes such as spheres, cubes, triangles and also polygons as seen in Fig. 2b. Ag nanoparticles acquired by the third process (sample 3) with 22 h of continuous stirring exhibited monodispersity with particle size 10 ± 2 nm. The monodispersed Ag nanoparticles are highly spherical as seen in Fig. 2c. Thus, by altering the stirring time, the dispersity of the particles could be controlled. The obtained polydispersed Ag nanoparticles are polycrystalline as the lattice orientation

changes within the particle as seen in Fig. 3a. Such change is not observed in the case of monodispersed Ag nanoparticles as seen in Fig. 3b confirming that these particles are single crystals.

FTIR spectrum

The FTIR spectra taken for all three samples are identical. The spectrum reveals the functional groups present in the sample (Fig. 4). The intense broad band at $3,386 \text{ cm}^{-1}$ is attributed to the hydroxy group, while $1,638 \text{ cm}^{-1}$ shows the C=C stretching. The band $1,051 \text{ cm}^{-1}$ corresponds to C–O stretch, while $2,926$ and 999 cm^{-1} are related to the C–H stretching and bending of the aromatic benzene rings, respectively. In the sample, the benzene rings are present in sodium benzoate, sodium methylparaben and sodium propylparaben. The band at $1,418 \text{ cm}^{-1}$ corresponds to the carboxylate (COO⁻) group which is also seen in the benzene ring. The wavenumbers $1,268$ and 929 cm^{-1} are related to the OH bending and 640 cm^{-1} shows the NO₂ vibrations associated with bronopol. Every 5 ml of gripe water used contains (as per its label) sodium bicarbonate (Sarjikakshara)—0.05 g, Dill oil (Anethum Graveolens)—0.005 ml, sugar—1.10 g with the preservatives bronopol, sodium benzoate, sodium methylparaben, and sodium propylparaben. FTIR spectrum concludes that sodium benzoate, sodium methylparaben, sodium propylparaben, and bronopol (also called as 2-bromo 2-nitropropane 1,3-diol) present in gripe water stabilize the silver nanoparticles.

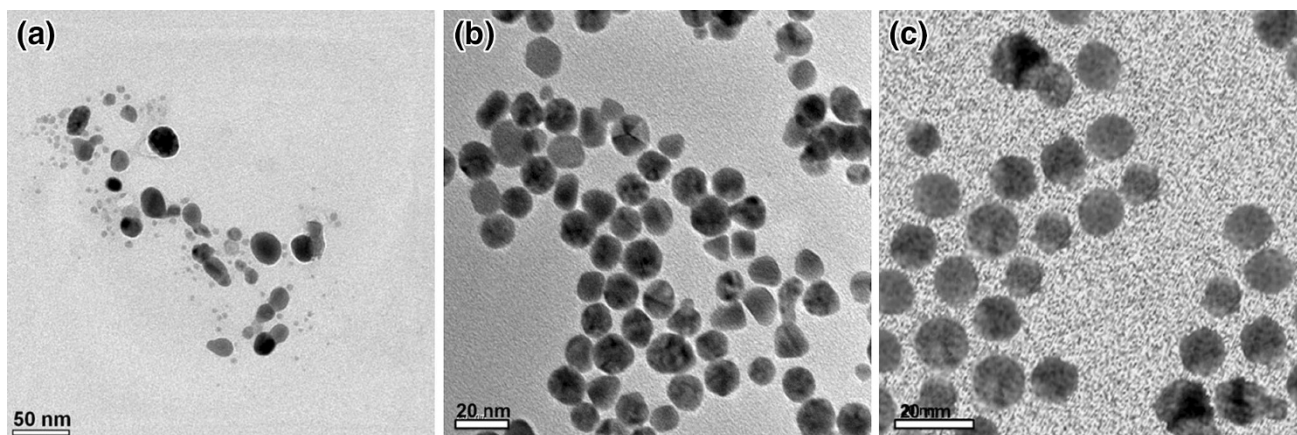


Fig. 2 **a** Polydispersed Ag nanoparticles (Sample 1) with particle size variation from 2 to 40 nm **b** polydispersed Ag nanoparticles (Sample 2) with particle size variation from 5 to 15 nm **c** Monodispersed Ag nanoparticles (Sample 3) with particle size variation from 8 to 12 nm

Fig. 3 **a** Lattice orientation within a single polydispersed Ag nanoparticle **b** lattice orientation within a single monodispersed Ag nanoparticle

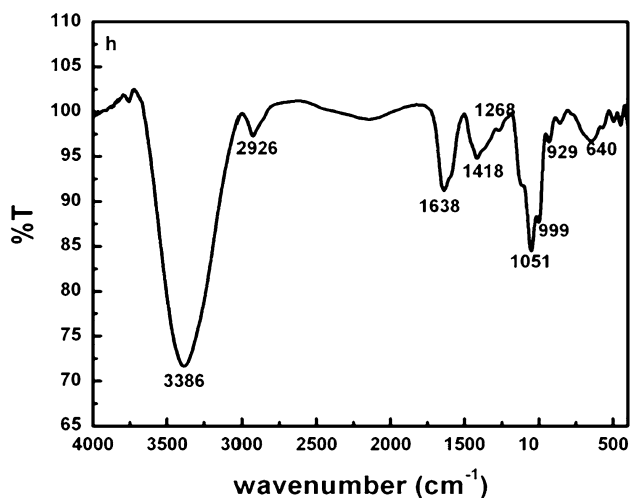
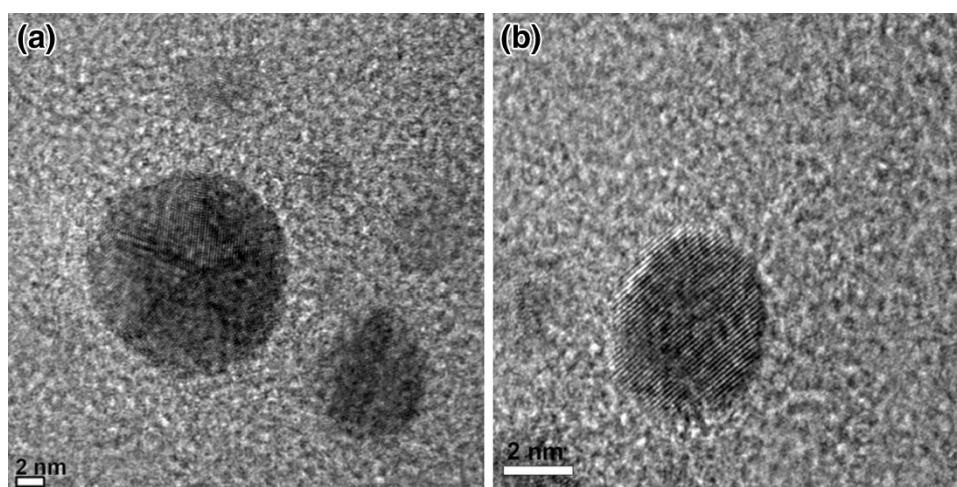


Fig. 4 FTIR Spectrum of Ag nanoparticles synthesized using gripe water

When the source solution of AgNO_3 is stirred with the gripe water, it acts as a reducing agent, i.e., gripe water breaks the bond and Ag^{1+} ions are formed. As more and more of these metal atoms form, the solution becomes supersaturated and the Ag gradually starts to grow in the form of sub-nanometer particles, which finally grows into nanoparticles and is stabilized by the same gripe water. The ingredients sodium bicarbonate and sucrose in gripe water act as reducing agents. These ingredients are tested as reducing agents separately and also they are reported earlier as reducing agents (Ayadi et al. 2013; Filippo et al. 2009). The other elements present in gripe water such as dill oil (*Anethum Graveolens*), sodium methylparaben, sodium propylparaben, sodium benzoate, 2-bromo 2-nitropropane 1,3-diol (bronopol) help in stabilizing the Ag nanoparticles. The color of the Ag nanoparticles is yellowish brown when synthesized. The SPR band of the nanoparticles recorded exactly after 90 days of synthesis

Fig. 5 Schematic representation of closed-aperture Z-scan set-up

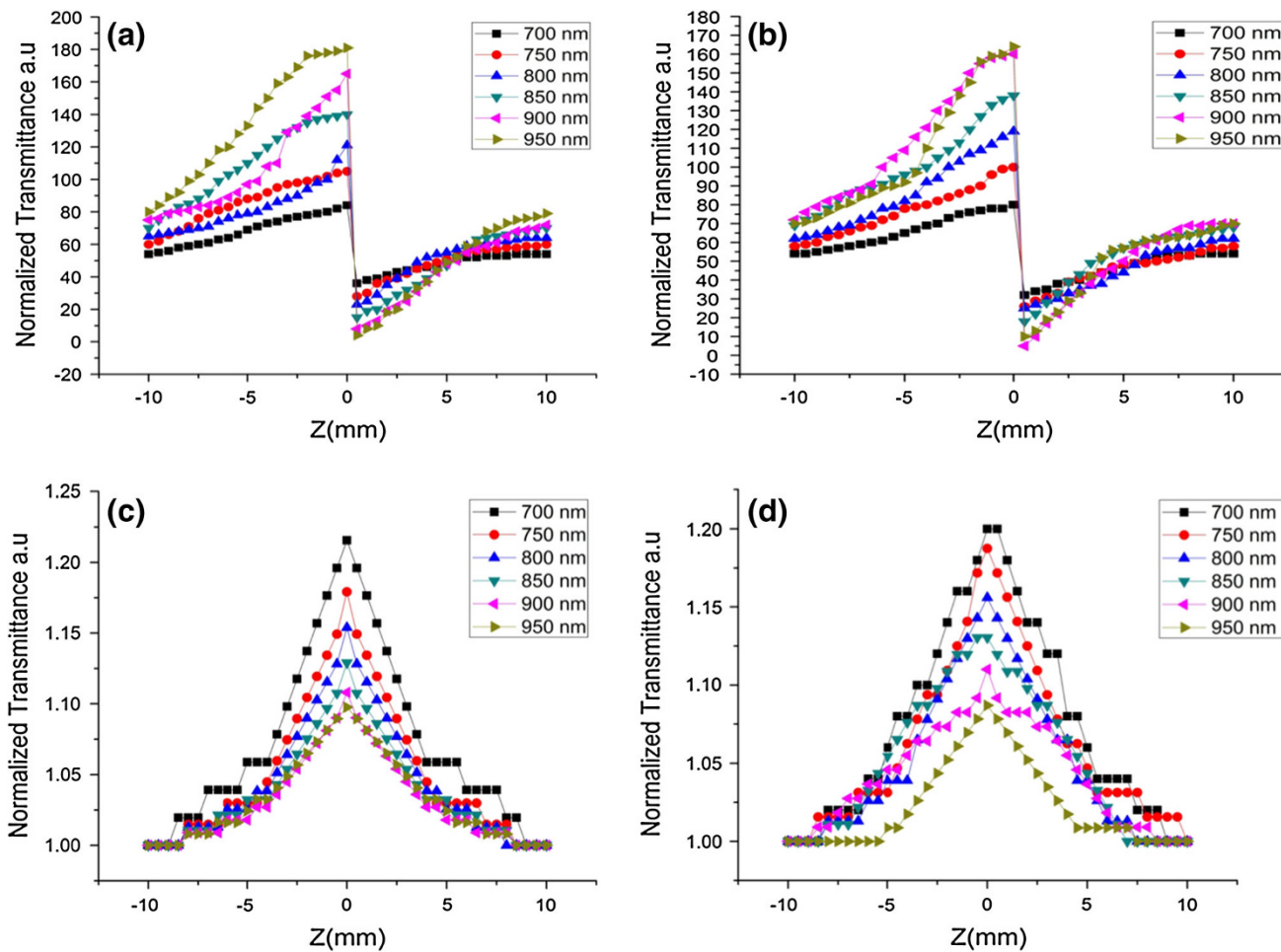
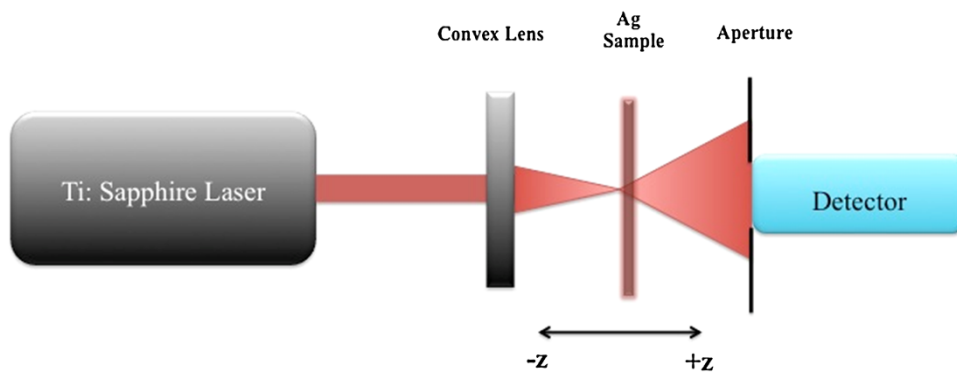


Fig. 6 **a** Closed-aperture Z-scan of monodispersed Ag nanoparticles at different wavelengths, **b** closed-aperture Z-scan of polydispersed Ag nanoparticles at different wavelengths, **c** open-aperture Z-scan

plot of monodispersed Ag nanoparticles at different wavelengths and **d** open-aperture Z-scan plot of polydispersed Ag nanoparticles at different wavelengths

does not show any shift or change indicating the stability of Ag nanoparticles. After 90 days period, black precipitates form gradually and the sample becomes colorless. UV–VIS spectrum taken does not show any band. Thus, it is inferred that the prepared nanoparticles are highly stable for 3 months at room temperature (25 °C).

Z-scan analysis

The nonlinear optical property was studied using single beam Z-scan technique. Sheik-Bahae et al. (1990) developed this method to measure the sign and magnitude of nonlinear refraction n_2 of a material. Both nonlinear

absorption and nonlinear refraction were determined using closed- and open-aperture Z-scans, respectively. The experimental schematic set-up of Z-scan is shown in Fig. 5. The colloidal Ag was taken in a quartz cuvette of width 1 mm and mounted on a translation stage. The cuvette with the Ag nanoparticles was moved across the focal region (+z to -z, i.e., -10 to +10 mm) along the direction of propagation of the laser beam.

The transmitted beam intensity was collected and measured through an aperture by a photodetector attached to the digital power meter. When the sample was moved towards the focus of the lens $z = 0$, the beam irradiance increased leading to pre-focal peak and when moved away from the focus, the beam irradiance decreased suddenly leading to post-focal valley (as seen in Fig. 6a, b). This indicates that the prepared Ag nanoparticles have negative nonlinearity. The nonlinear refractive index (n_2) is calculated using the standard relations (Bahae et al. 1990; Cassano et al. 2001) given by Eqs. 1 and 2.

$$n_2 = \frac{\Delta\Phi_0}{kL_{\text{eff}}I_0} \quad (1)$$

where n_2 is the nonlinear refractive index, k is the wave number ($k = 2\pi/\lambda$) and $\Delta\Phi_0$ is the on-axis phase shift at the focus. I_0 is the peak intensity within the sample at the focus. L_{eff} is the effective thickness of the sample (1 mm).

$$\Delta\Phi_0 = \frac{\Delta T_{p-v}}{0.406(1-S)^{0.25}} \quad (2)$$

S is the linear aperture transmittance (0.5) and ΔT_{p-v} is the normalized peak valley difference obtained from the closed-aperture Z-scan trace. Nonlinear absorption coefficient β of the prepared Ag nanoparticles is obtained from open-aperture Z-scan using Eq. 3. In this set-up, the aperture was removed as the name suggests and the entire beam was focused into the detector through a lens.

$$\beta = \frac{2\sqrt{2}\Delta T}{I_0L_{\text{eff}}} \quad (3)$$

$\Delta T = I - T_p$, where T_p is the normalized peak value from the open-aperture plot. Figure 6a shows the closed-aperture Z-scan trace of monodispersed Ag nanoparticles for different incident wavelengths from 700 to 950 nm.

Third-order nonlinear susceptibility χ^3 of the nanoparticles was obtained using the relations as in Eqs. 4, 5 and 6, (Prakash et al. 2002).

$$(\chi^3) = \sqrt{\{\text{Re}(\chi^3)^2 + \text{Im}(\chi^3)^2\}} \quad (4)$$

$$\text{Re}(\chi^3) = \frac{\varepsilon_0 c^2 10^{-4} n_0^2}{\pi} \times n_2 \quad (5)$$

$$\text{Im}(\chi^3)' = \frac{\varepsilon_0 c^2 n_0^2 10^{-2} \lambda}{4\pi^2} \times \beta \quad (6)$$

where, $\varepsilon_0 = 8.854 \times 10^{-14}$ F/m is the vacuum permittivity, c is the speed of light in vacuum (3×10^{10} cm/sec) and n_0 is the linear refractive index (1.33). The real part $\text{Re}(\chi^3)$ is proportional to the nonlinear refractive index of the nanoparticles, while the imaginary part $\text{Im}(\chi^3)'$ is proportional to the nonlinear absorption coefficient β . The measured nonlinear parameters of the prepared Ag nanoparticles are tabulated in Table 1.

The Z-Scan plots, both closed and open aperture are illustrated in Fig. 6. The prepared silver nanoparticles (both monodispersed and polydispersed) indicate negative nonlinearity as their closed-aperture Z-scan traces show peak followed by valley. The nonlinear refractive index n_2 of the nanoparticles is in the order of 10^{-8} cm²/W. The n_2 value increases from 1.44 to 4.87×10^{-8} cm²/W with increase in the incident wavelength for the monodispersed Ag nanoparticles and a similar increase for the polydispersed nanoparticles is noted from 1.44 to 4.84×10^{-8} cm²/W. The concentration of the as-synthesized monodispersed Ag nanoparticles obtained from inductive coupled plasma (ICP) is 0.274 mol/L and for the polydispersed Ag nanoparticles the concentration is 0.280 mol/L. The nonlinear refractive index n_2 also varies with concentration of the nanoparticles. The variation of n_2 with concentration is given in supplementary information.

The nonlinear absorption coefficient β is obtained from the open-aperture Z-scan. From the open-aperture Z-scan, it is seen that the nonlinear absorption of silver nanoparticles decreases from 2.94 to 1.26×10^{-4} cm/W for the monodispersed Ag nanoparticles of concentration 0.274 mol/L with increase in wavelength. In the case of polydispersed Ag nanoparticles with a concentration of 0.280 mol/L, the β value decreases from 2.8 to 1.4×10^{-4} cm/W. From the single beam Z-scan technique, it is seen that the nonlinear refractive index n_2 of the silver nanoparticles increases with increase in wavelength while the absorption coefficient β as well as the third-order nonlinear susceptibility χ^3 decrease. The variation of n_2 , β and χ^3 with wavelength is shown in Fig. 7.

SERS analysis

In general, the SERS studies are performed by coating the molecule to be studied as a probe and the metal nanoparticles as analyte on a substrate. This leads to areas called hot-spots at which large enhancement occurs at the junctions between the nanoparticles. The hot-spots can be defined as the regions where the enhancement is increased manifold due to a number of factors (Nie and Emory 1997). Due to the presence of hot-spots, certain peaks of the molecule show huge enhancements due to the single molecule enhancement. However, in this case there are no such

Table 1 Measured nonlinear parameters of monodispersed AgNps of concentration 0.274 mol/L and polydispersed AgNps of concentration 0.280 mol/L

λ (nm)	ΔT_{p-v}	$\Delta\Phi_o$	$n_2 \times 10^{-8}$ cm ² /W	$\beta \times 10^{-4}$ cm/W	$\text{Re}(\chi^3) \times 10^{-2}$ (esu)	$\text{Im}(\chi^3)' \times 10^{-7}$ (esu)	$\chi^3 \times 10^{-9}$ (esu)
Monodispersed AgNps							
700	0.88	2.60	1.44	2.94	0.06	0.21	0.06
750	1.28	3.76	2.23	2.38	1.00	0.18	1.00
800	1.50	4.41	2.80	2.10	1.25	0.17	1.25
850	1.78	5.23	3.52	1.68	1.57	0.14	1.57
900	2.09	6.13	4.37	1.40	1.95	0.13	1.95
950	2.21	6.47	4.87	1.26	2.18	0.12	2.18
Polydispersed AgNps							
700	0.88	2.60	1.44	2.80	0.06	0.20	0.06
750	1.27	3.73	2.22	2.52	0.99	0.19	0.99
800	1.51	4.44	2.81	2.10	1.26	0.17	1.26
850	1.74	5.09	3.43	1.82	1.53	0.15	1.53
900	2.15	6.30	4.49	1.54	2.01	0.14	2.01
950	2.20	6.44	4.84	1.40	2.17	0.13	2.17

λ wavelength, ΔT_{p-v} normalized peak valley difference, n_2 nonlinear refractive index, β nonlinear absorption coefficient, $\text{Re}(\chi^3)$ real part of χ^3 , $\text{Im}(\chi^3)'$ imaginary part of χ^3 , χ^3 third-order nonlinear susceptibility

constraints as the whole experiment was carried out in liquid phase in a cuvette. The nanoparticles were taken in colloidal form and the probe R6G was in solution phase. This leads to the enhancement of all the peaks of R6G. The enhancement factor was calculated as an average enhancement over all the peaks obtained in the spectrum. The SERS of rhodamine 6G using polydispersed and monodispersed Ag nanoparticles is exhibited in Fig. 8 and the calculated enhancement factors are tabulated in Table 2.

The concentration of the dye R6G taken was very low as high concentrations led to blinding of the Raman signals. Equal volume ratio of R6G (1×10^{-12} M) and nanoparticles was taken in a quartz cuvette for the analysis as this ratio yielded the maximum enhancement of Raman signal of the dye. The key parameter that defines SERS is the enhancement factor (EF). It is defined as the ratio of the enhancement obtained to what would be obtained for the same molecule in non-SERS conditions. The average SERS EF was calculated according to the formula in Eq. 7 (Wang et al. 2014).

$$\text{EF} = \frac{I_{\text{SERS}} N_0}{I_0 N_{\text{SERS}}} \quad (7)$$

where I_0 and I_{SERS} are the peak intensities of the Raman measurement under normal and SERS conditions, respectively. N_0 and N_{SERS} are the number of R6G molecules in the scattering volume for the normal Raman measurement and SERS measurement correspondingly. The vibrational modes of the R6G dye are in the range of 1,800–600 cm⁻¹. The vibrational bands observed in the R6G spectra from

1,314 to 1,651 cm⁻¹ are due to the aromatic C–C stretching. The other wavenumber 1,124 cm⁻¹ is a weak band due to the C–H (ip) bend, while 774 cm⁻¹ arises from the C–H (oop) bend and 614 cm⁻¹ is due to C–C–C (ip) bend (Vosgrone and Meixner 2005).

SPR spectra recorded for R6G with addition of pure gripe water are not showing any enhancement of Raman spectra, whereas addition of Ag nanoparticles synthesized using gripe water results in enhancement in the order of 10⁹. From the SERS spectrum, it is deduced that the large enhancements are observed with increase in dispersity of the nanoparticles. Polydispersed nanoparticles consist of shapes such as spheres, cubes, triangles, hexagons, pentagons and other polygons. Since the shape and dimensions of Ag nanoparticles have an influence on the surface plasmon resonance of the nanoparticles, it also has an effect on the enhancement of Raman spectrum.

Conclusion

In summary, we have developed a complete green methodology for the synthesis of silver nanoparticles using gripe water as reducing as well as stabilizing agent. The dispersity of the nanoparticles could be controlled by this method as both monodispersed and polydispersed particles were obtained in one step with great ease. The prepared nanoparticles are highly stable for more than 2 months at room temperature (25 °C). The as-prepared Ag nanoparticles exhibit good optical nonlinear properties. The optical nonlinear refractive index variation of the nanoparticles

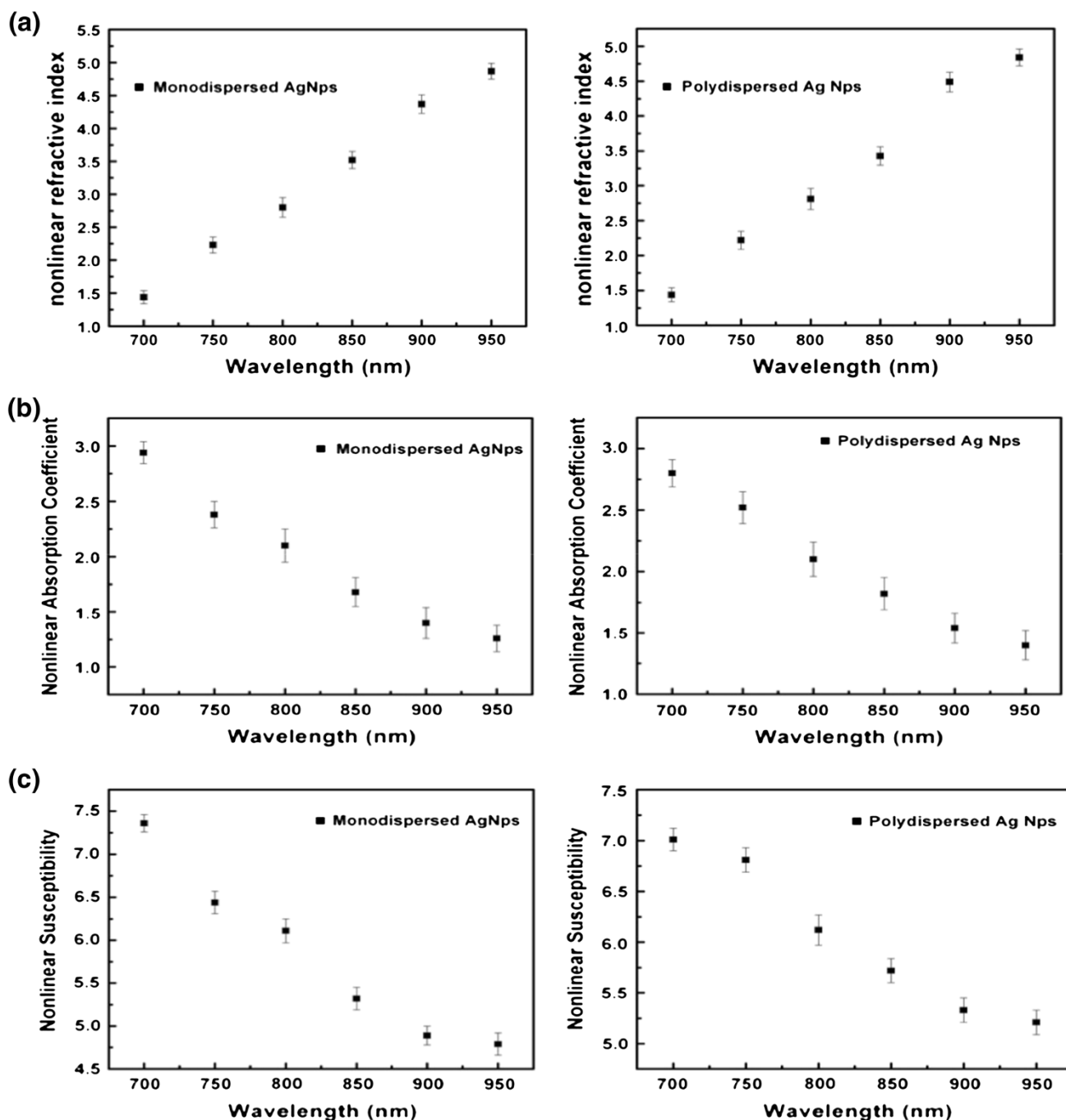


Fig. 7 **a** Variation of nonlinear refractive index of Ag nanoparticle with wavelength; **b** variation of nonlinear absorption coefficient of Ag nanoparticles with wavelength; **c** variation of nonlinear susceptibility of Ag nanoparticle with wavelength

was studied using tunable mode-locked Ti:Sapphire laser with a pulse width of 160 fs by varying the wavelength from 700 to 950 nm. The optical nonlinearity of the nanoparticles increases with increase in wavelength. The nonlinear refractive index n_2 is found to be in the order of 10^{-8} cm²/W, nonlinear absorption coefficient β is obtained in the order of 10^{-4} cm/W and the third-order nonlinear susceptibility χ^3 is in the order of 10^{-9} (esu). The SERS

behavior of the nanoparticles is also studied using dye rhodamine 6G. All the nine predominant peaks of the dye are enhanced by the Ag nanoparticles and the enhancement factor obtained is high in the order of 10^9 . The dispersity of the nanoparticles also plays a vital role in this SERS phenomenon as the polydispersed particles offer more enhancement than the monodispersed nanoparticles. Hence, this study proves to be an excellent tool for the

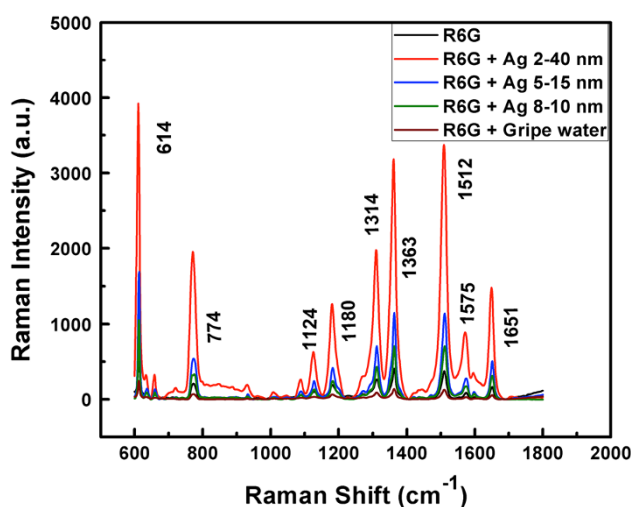


Fig. 8 Surface enhanced Raman spectrum of rhodamine 6G using Ag nanoparticles

Table 2 Calculated average enhancement factors of R6G polydispersed and monodispersed Ag nanoparticles

Ag nanoparticle	Average enhancement factor
Polydispersed (2–40 nm)	8.16×10^9
Polydispersed (5–15 nm)	2.79×10^9
Monodispersed (8–10 nm)	1.67×10^9

enhancement of Raman signals and can be extended for biosensing.

Acknowledgments Author P. K. Palanisamy acknowledges the Emeritus fellowship award of University Grants Commission (UGC), New Delhi.

Open Access This article is distributed under the terms of the Creative Commons Attribution License which permits any use, distribution, and reproduction in any medium, provided the original author(s) and the source are credited.

References

- Anker JN, Hall WP, Lyandres O, Shah NC, Zhao J, Duyn RPV (2008) Biosensing with plasmonic nanosensors. *Nat Mater* 7:442–453
- Atiyeh BS, Costagliola M, Hayek SN, Dibo SA (2007) Effect of silver on burn wound infection control and healing: review of the literature. *Burns* 33:139–148
- Augustine R, Nandakumar K, Thomas S (2013) A facile and rapid method for the black pepper leaf mediated green synthesis of silver nanoparticles and the antimicrobial study. *Appl Nanosci*. doi:10.1007/s13204-013-0260-7
- Ayadi S, Perca C, Legrand L (2013) New one-pot synthesis of Au and Ag nanoparticles using green rust reactive particle as a micro-reactor. *Nanoscale Res Lett* 8:95

- Bahae SM, Said AA, Wei TH, Hagan DJ, Stryland EWV (1990) Sensitive measurement of optical nonlinearities using a single beam. *IEEE J Quantum Electron* 26:760–768
- Blumenthal I (2000) The gripe water story. *J R Soc Med* 93:172–174
- Cassano T, Tommasi R, Ferrara M, Babudri F, Farinola GM, Naso F (2001) Substituent-dependence of the optical nonlinearities in poly(2,5-dialkoxy-*p*-phenylenevinylene) polymers investigated by the Z-scan technique. *Chem Phys* 272:111–118
- Dauthal P, Mukhopadhyay M (2013) In-vitro free radical scavenging activity of biosynthesized gold and silver nanoparticles using *Prunus armeniaca* (apricot) fruit extract. *J Nanopart Res* 15:1366–1376
- Dong X, Ji X, Jing J, Li M, Li J, Yang W (2010) Synthesis of triangular silver nanoprisms by stepwise reduction of sodium borohydride and trisodium citrate. *J Phys Chem C* 114:2070–2074
- El-Sayed IH, Huang X, El-Sayed MA (2005) Surface plasmon resonance scattering and absorption of anti-EGFR antibody conjugated gold nanoparticles in cancer diagnostics: applications in oral cancer. *Nano Lett* 5:829–834
- Filippo E, Serra A, Buccolieri A, Manno D (2009) Green synthesis of silver nanoparticles with sucrose and maltose: morphological and structural characterization. *J Non Cryst Solids* 356:344–350
- Fleishman M, Hendra PJ, McQuillan AJ (1974) Raman spectra of pyridine adsorbed at a silver electrode. *Chem Phys Lett* 26:163–166
- Honary S, Barabadi H, Fathabad EG, Naghibi F (2013) Green synthesis of silver nanoparticles induced by the fungus *penicillium citrinum*. *Trop J Pharm Res* 12:7–11
- Janmaire DL, Duyn RPV (1977) Surface raman spectroelectrochemistry. *Electroanal Chem* 84:1–20
- Jeyaraj M, Sathishkumar G, MubarakAli D, Rajesh M, Arun R, Kapildev G, Manickavasagam M, Thajuddin N, Premkumar K, Ganapathi A (2013) Biogenic silver nanoparticles for cancer treatment: an experimental report. *Colloids Surf B Biointerfaces* 106:86–92
- Junhua Y, Choi S, Dickson RM (2009) Shuttle-based fluorogenic silver-cluster biolabels. *Angew Chem* 2:324–326
- Kelly KL, Coronado E, Zhao LL, Schatz GC (2003) The optical properties of metal nanoparticles: the influence of size, shape, and dielectric environment. *J Phys Chem* 107:668–677
- Kirubha E, Palanisamy PK (2013) Gripe water as reducing and stabilizing agent for synthesis of size controlled gold nanoparticles. *J Nanosci Nanotechnol* 13:2289–2294
- Lakshmiipathy R, Reddy BP, Sarada NC, Chidambaram K, Pasha SK (2014) Watermelon rind-mediated green synthesis of noble palladium nanoparticles: catalytic application. *Appl Nanosci*. doi:10.1007/s13204-014-0309-2
- Liong M, Lu J, Kovochich M, Xia T, Ruehm SG, Nel AE, Tamanoi F, Zink JI (2008) Multifunctional inorganic nanoparticles for imaging, targeting, and drug delivery. *ACS Nano* 2:889–896
- Mafuné F, Kohno J, Takeda Y, Kondow T (2000) Structure and stability of silver nanoparticles in aqueous solution produced by laser ablation. *J Phys Chem B* 104:8333–8337
- Maier SA, Kik PG, Atwater HA, Meltzer S, Harel E, Koel BE, Requicha AAG (2003) Local detection of electromagnetic energy transport below the diffraction limit in metal nanoparticle plasmon waveguides. *Nat Mater* 2:229–232
- Majumdar R, Bag BG (2013) *Acacia nilotica* (Babool) leaf extract mediated size controlled rapid synthesis of gold nanoparticles and study of its catalytic activity. *Int Nano Lett*. doi:10.1186/2228-5326-3-53
- Mohanpuria P, Nisha K, Yadav RSK (2008) Biosynthesis of nanoparticles: technological concepts and future applications. *J Nanopart Res* 10:507–517

- Moskovits M (2005) Surface-enhanced Raman spectroscopy: a brief retrospective. *J Raman Spectrosc* 36:485–496
- Nie SM, Emory SR (1997) Probing single molecules and single nanoparticles by surface-enhanced Raman scattering. *Science* 275:1102–1106
- Philip D (2010) In-vitro free radical scavenging activity of biosynthesized gold and silver nanoparticles using *Prunus armeniaca* (apricot) fruit extract. *Physica E* 42:1417–1424
- Pourjavadi A, Soleyman R (2011) Novel silver nano-wedges for killing microorganisms. *J Nanopart Res* 13:4647–4658
- Prakash GV, Cazzanelli M, Gaburro Z, Pavesi L (2002) Nonlinear optical properties of silicon nanocrystals grown by plasma-enhanced chemical vapor deposition. *J Appl Phys* 91:4607–4610
- Raveendran P, Fu J, Wallen SL (2003) Completely green synthesis and stabilization of metal nanoparticles. *J Am Chem Soc* 125:13940–13941
- Singh M, Kalaivani R, Manikandan S, Sangeetha N, Kumaraguru AK (2013) Facile green synthesis of variable metallic gold nanoparticle using *Padina gymnospora*, a brown marine macroalga. *Appl Nanosci* 3:145–151
- Sun Y, Xia Y (2002) Shape-controlled synthesis of gold and silver nanoparticles. *Science* 298:2176–2179
- Swamy MK, Sudipta KM, Jayanta K, Balasubramanya S (2014) The green synthesis, characterization, and evaluation of the biological activities of silver nanoparticles synthesized from *Leptadenia reticulata* leaf extract. *Appl Nanosci*. doi:10.1007/s13204-014-0293-6
- Vankar PS, Shukla D (2012) Biosynthesis of silver nanoparticles using lemon leaves extract and its application for antimicrobial finish on fabric. *Appl Nanosci* 2:163–168
- Venkatesham M, Ayodhya D, Madhusudhan A, Babu NV, Veerabhadram G (2014) A novel green one-step synthesis of silver nanoparticles using chitosan: catalytic activity and antimicrobial studies. *Appl Nanosci* 4:113–119
- Vosgrone T, Meixner AJ (2005) Surface- and resonance-enhanced micro-Raman spectroscopy of xanthene dyes: from the ensemble to single molecules. *Chem Phys Chem* 6:154–163
- Wang T, Zhang Z, Liao F, Cai Q, Li Y, Lee ST, Shao M (2014) The effect of dielectric constants on noble metal/semiconductor SERS enhancement: FDTD simulation and experiment validation of Ag/Ge and Ag/Si substrates. *Nature* 4:4052–4059